An EPR study of the phase transitions and Gd^{3+} zero-field splitting parameters in $RbR(SO_4)_2.4H_2O$ (R = Er, Dy, Pr, Nd, Sm, Eu)

1998 J. Phys.: Condens. Matter 10 10667

(http://iopscience.iop.org/0953-8984/10/47/017)

J. Phys.: Condens. Matter **10** (1998) 10667–10677. Printed in the UK PII: S0953-8984(98)93203-9

An EPR study of the phase transitions and Gd^{3+} zero-field splitting parameters in $RbR(SO_4)_2.4H_2O$ (R = Er, Dy, Pr, Nd, Sm, Eu)

Sushil K Misra, Samih Isber† and Lin Li

Physics Department, Concordia University, 1455 de Maisonneuve Boulvard West, Montreal, Quebec, H3G 1M8 Canada

Received 8 April 1998, in final form 28 August 1998

Abstract. X-band (∼9.6 GHz) electron paramagnetic resonance measurements were carried out on Gd^{3+}-doped $RbEr(SO_4)_2.4H_2O$ and $RbDy(SO_4)_2.4H_2O$ single crystals in the 4.2–295 K temperature range, and on Gd^{3+}-doped $RbPr(SO_4)_2.4H_2O$, $RbNd(SO_4)_2.4H_2O$, $RbSm(SO_4)_2.4H_2O$ and $RbEu(SO_4)_2.4H_2O$ single crystals in the 4.2–110 K range. Gd^{3+} room-temperature spin-Hamiltonian parameters were estimated in $RbR(SO_4)_2.4H_2O$ samples with R = Er, Dy. The following phase transitions undergone by the various host crystals were found to occur: three second-order phase transitions in $RbDy(SO_4)_2.4H_2O$ at 260.3 K, 226.9 K and 65.4 K, and second-order and first-order phase transitions in $RbEr(SO_4)_2.4H_2O$ at 228.1 and 68.8 K, respectively. In addition, there were observed first-order phase transitions in each of $RbNd(SO_4)_2.4H_2O$ (at 72.1 K), $RbSm(SO_4)_2.4H_2O$ (at 70.3 K) and $RbEu(SO_4)_2.4H_2O$ (at 79.4 K), and two in $RbPr(SO_4)_2.4H_2O$ (at 71.4 and 9.7 K) crystals, in the 4.2–110 K range, in addition to those reported previously in the 110–295 K range. Systematics of the various phase transitions occurring in $RbR(SO_4)_2.4H_2O$ (R = Pr, Nd, Sm, Er, Dy, Eu) single crystals in the temperature range 4.2–295 K, and those of Gd^{3+} zero-field splitting parameters at room temperature, have been deduced.

1. Introduction

Electron paramagnetic resonance (EPR) measurements have been extensively used to study local environment, and to estimate spin-Hamiltonian parameters of probe transition-metal ions in host crystals [1–5]. Phase transitions undergone by host crystals produce dynamic effects which affect zero-field splitting (ZFS), width and intensity of EPR lines of the probe ion. Since the rare-earth ions Pr^{3+}, Nd^{3+}, Sm^{3+}, Dy^{3+} and Er^{3+} have rather short spin–lattice relaxation times above 77 K, their EPR spectra cannot be observed in the convenient temperature range achieved with liquid nitrogen. On the other hand, EPR spectrum for the Gd^{3+} ion can be easily recorded over an extended temperature range from liquid-helium temperature up to room temperature, rendering this ion as a useful probe to study properties of the host $RbR(SO_4)_2.4H_2O$ (R = rare earth) crystals. To this end, one uses a rather small fraction of the probe Gd^{3+} ion (<1%) to minimize the distortion of the lattice caused by the different size of the Gd^{3+} ion from those of the host rare-earth ions (R = Er^{3+}, Dy^{3+}, Pr^{3+}, Nd^{3+}, Sm^{3+} and Eu^{2+}).

† Present address: Physics Department, American University of Beirut, Bliss Street, PO Box 11-0236, Beirut, Lebanon.

0953-8984/98/4710667+11$19.50

Various experimental techniques, e.g., infrared reflectivity, specific heat, x-ray, neutron scattering and nuclear magnetic resonance, have been used to study phase transitions in $RbR(SO_4)_2.4H_2O$ crystals. Recently, Jasty and Malhotra [6] reported specific heat and x-ray measurements on a similar family of crystals, $NH_4R(SO_4)_2.4H_2O$, and detected two phase transitions in the temperature range 100–295 K.

EPR studies on four Gd^{3+}-doped $RbR(SO_4)_2.4H_2O$ crystals (R = Pr, Nd, Eu, Sm) in the temperature range 110–295 K to study phase transitions, and to estimate Gd^{3+} spin-Hamiltonian parameters (SHPs) in these crystals at room temperature, were recently published [7]. The purpose of the present paper is to report EPR studies on (i) Gd^{3+}-doped $RbEr(SO_4)_2.4H_2O$ and $RbDy(SO_4)_2.4H_2O$ crystals over the entire 4.2–295 K temperature range; and (ii) to extend the temperature range of phase-transition study on Gd^{3+}-doped $RbR(SO_4)_2.4H_2O$ (R = Pr, Nd, Eu, Sm) crystals from 110–295 K to 4.2–110 K, in order to study the systematics of the phase transitions undergone by $RbR(SO_4)_2.4H_2O$ crystals, as well as those of Gd^{3+} zero-field splitting parameters in these crystals. The EPR spectra will here be exploited to determine the temperatures, and natures of the phase transitions, and to estimate room-temperature spin-Hamiltonian parameters (SHP) in the samples with R = Dy, Er. (SHP cannot be estimated below the phase-transition temperature because the site symmetry changes below the phase-transition temperature, as is the case of the crystals with R = Sm, Nd, Pr, Eu [7].)

2. EPR spectra and natures of phase transitions

An X-band Bruker EPR spectrometer equipped with an Oxford Instruments helium gas-flow cryostat was used to measure single-crystal EPR spectra down to about 4 K. The sample dimensions used in the present study were about $0.5 \times 0.5 \times 1$ mm^3.

2.1. $RbR(SO_4)_2.4H_2O$ (R = Dy, Er) in the range 4.2–295 K

The powder spectra exhibit fifteen lines indicating the presence of two magnetically inequivalent Gd^{3+} sites in the unit cell of $RbDy(SO_4)_2.4H_2O$ and $RbEr(SO_4)_2.4H_2O$, both characterized by monoclinic site symmetry possessing a twofold axis of symmetry, as revealed by the angular variation of EPR line positions. (These are hereafter referred to as sites I and II.) Single-crystal room-temperature Gd^{3+} EPR spectra in $RbEr(SO_4)_2.4H_2O$ and $RbDy(SO_4)_2.4H_2O$ are shown in figures 1(a) and 1(b), respectively. (The magnetic axes are defined to be those orientations of $\boldsymbol{B}$ at which extrema of EPR line positions are observed, the overall splitting decreasing in the order $\boldsymbol{B} \parallel Z, X, Y$.) Figure 2 exhibits the temperature variation of the EPR spectrum for Gd^{3+} in $RbDy(SO_4)_2.4H_2O$ for the orientation of the external magnetic field $\boldsymbol{B} \parallel Z$-axis at selected temperatures in the 4–295 K range; a similar variation, not shown here, is found in $RbEr(SO_4)_2.4H_2O$. Figure 2 reveals that Gd^{3+} zero-field splitting increases with decreasing temperature in both crystals. The angular difference between the maxima of the highest- and next-to-highest-field line, typical of monoclinic site symmetry [7], for the orientation of the external magnetic field, $\boldsymbol{B}$, in the ZX-plane for the Gd^{3+} ion in site I is about 4 degrees in both $RbDy(SO_4)_2.4H_2O$ and $RbEr(SO_4)_2.4H_2O$; this difference is larger for the Gd^{3+} ion at site II, being 17 and 20° for $RbEr(SO_4)_2.4H_2O$ and $RbDy(SO_4)_2.4H_2O$, respectively. This is similar to the situation in $NH_4R(SO_4)_2.4H_2O$ (R = Er, Nd, Sm), where the deviation increases in the sequence R = Er, Nd [7–9].

For $RbEr(SO_4)_2.4H_2O$, the position and width of the highest-field line at various temperatures in the 4.2–295 K range are shown in figure 3. Since the variations in the width and positions of EPR lines in $RbEr(SO_4)_2.4H_2O$ are gradual at 228.1 K, a second-order

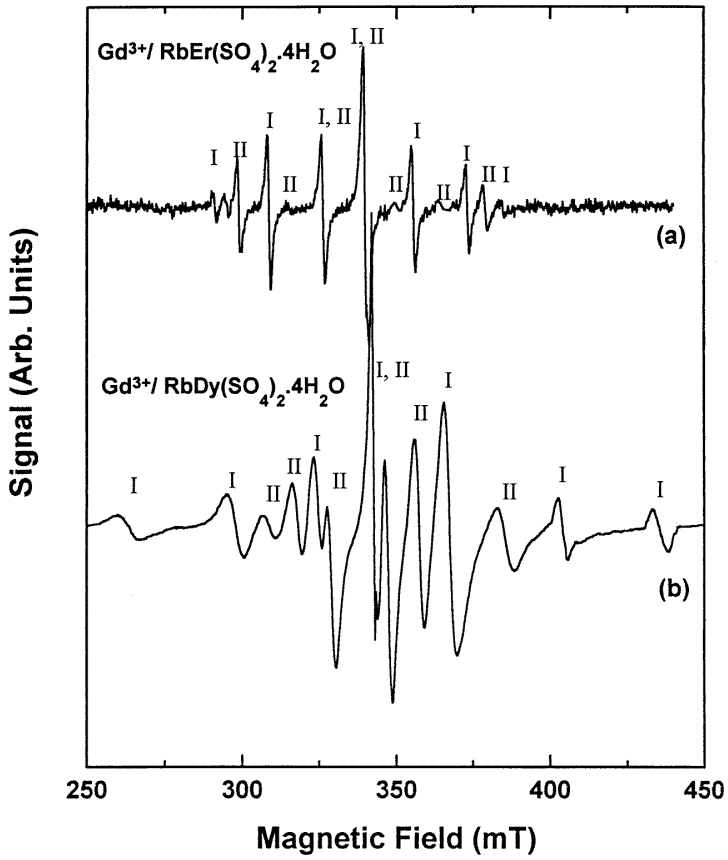

Figure 1. Room-temperature X-band (∼9.60 GHz) EPR spectra of (a) Gd^{3+} in $RbEr(SO_4)_2.4H_2O$, (b) Gd^{3+} in $RbDy(SO_4)_2.4H_2O$ as recorded for $\boldsymbol{B} \parallel Z$-axis. The Gd^{3+} EPR lines corresponding to sites I and II have been indicated.

phase transition is deduced to occur at this temperature, while these variations are abrupt at 68.8 K, implying the occurrence of a first-order phase transition at 68.8 K. These transition temperatures are in conformity with those found by the temperature dependence of the magnetic fields defining the positions of EPR lines. Below 68.8 K, the EPR linewidth remained invariant with temperature. The variation of width and position of the highest-field EPR line with temperature for $RbDy(SO_4)_2.4H_2O$ are shown in figure 4, an inspection of which reveals occurrences of three phase transitions, as deduced from the behaviour of the linewidths and line positions: at $T_c = 260.3$ K, $T_{c1} = 226.9$ K and $T_{c2} = 65.4$ K. All these transitions are deduced to be of second order, using the criterion that changes in widths and positions of EPR lines are gradual upon passing through the phase transition of second order, while they are abrupt upon passing through phase transitions of first order.

The first-derivative peak-to-peak Gd^{3+} EPR linewidths, ΔB_{PP}, for site II are, in general, larger than those for site I in the crystals with R = Dy and Er. At room temperature, the values of ΔB_{PP} for the various lines are 12–15 Gauss and 16–20 Gauss for sites I and II, respectively, in $RbEr(SO_4)_2.4H_2O$, while they are 40–50 Gauss and 50–60 Gauss for sites I and II, respectively, in $RbDy(SO_4)_2.4H_2O$. ΔB_{PP} are found to depend upon temperature, the

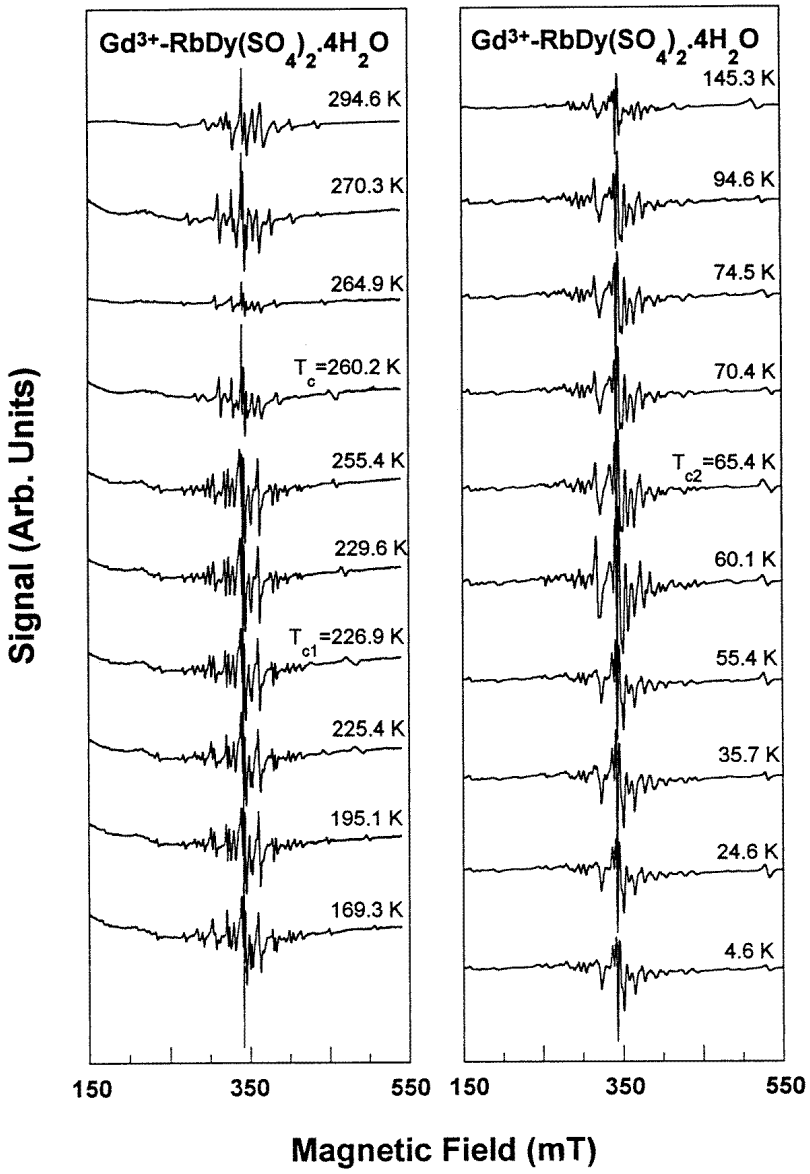

Figure 2. X-band (∼9.60 GHz) Gd^{3+} EPR spectra at selected temperatures for the orientation of the external magnetic field $\boldsymbol{B} \parallel Z$-axis in $RbDy(SO_4)_2.4H_2O$ single crystals at various temperatures in the 4.2–295 K temperature range to monitor the changes when the temperature is lowered.

lines becoming quite broad in the vicinity of a phase transition for both $RbDy(SO_4)_2.4H_2O$ and $RbEr(SO_4)_2.4H_2O$. The various phase-transition temperatures, and their natures, are listed in table 1.

Below the phase-transition temperatures of 228 K and 260 K, the symmetry at the Gd^{3+} site in $RbEr(SO_4)_2.4H_2O$ and $RbDy(SO_4)_2.4H_2O$, respectively, was found to be lower than monoclinic, as deduced from the angular variation of Gd^{3+} EPR line positions.

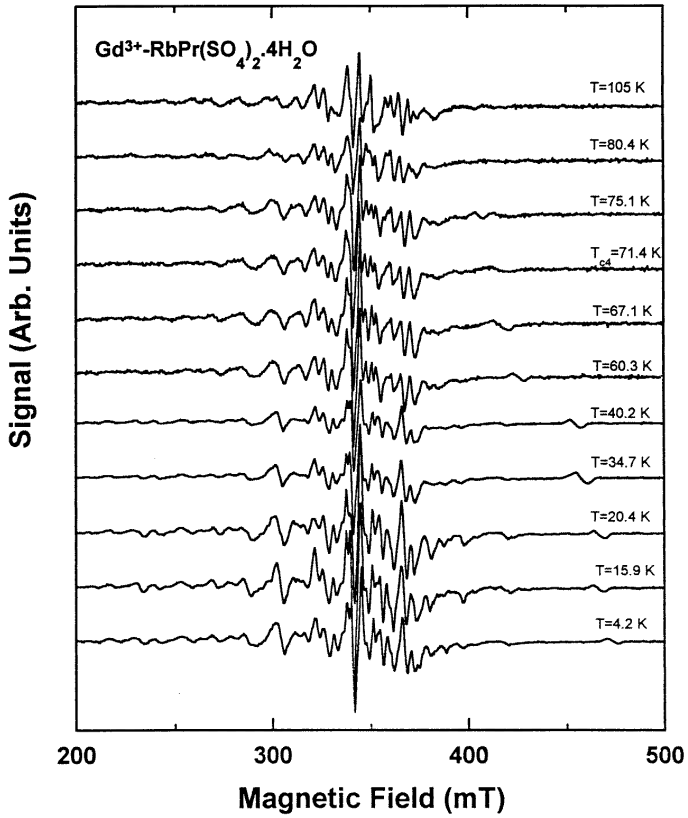

Figure 3. The position and width of the highest-field Gd^{3+} EPR line at X band (∼9.60 GHz) as functions of temperature for the external magnetic field orientation being parallel to the Z-axis in $RbEr(SO_4)_2.4H_2O$ in the 4.2–295 K temperature range.

2.2. $RbR(SO_4)_2.4\,H_2O$ ($R = Pr$, Nd, Sm, Eu) in the range 4.2–110 K

For these host crystals, figure 5 shows selected Gd^{3+} EPR spectra in $RbPr(SO_4)_2.4H_2O$ (in $RbEu(SO_4)_2.4H_2O$ a similar figure is found), and figure 6 exhibits the widths and positions of EPR lines of the highest-field line in $RbEu(SO_4)_2.4H_2O$ below 110 K. (In $RbPr(SO_4)_2.4H_2O$ a similar figure is found.) There is found second first-order phase transition in each of $RbPr(SO_4)_2.4H_2O$, $RbNd(SO_4)_2.4H_2O$, $RbSm(SO_4)_2.4H_2O$ and $RbEu(SO_4)_2.4H_2O$ crystals at 71.4 K (R = Pr), 72.1 K (R = Nd), 70.3 K (R = Sm) and 79.4 K (R = Eu) as revealed by gradual changes in linewidths and line positions. In addition $RbPr(SO_4)_2.4H_2O$ undergoes one more second-order phase transition at 9.7 K.

3. Spin Hamiltonian

The Gd^{3+} spin Hamiltonian appropriate to the monoclinic site symmetry, with the twofold symmetry axis $C_2 \parallel Z$-axis, in $RbR(SO_4)_2.4H_2O$ (R = Dy, Er, Pr, Nd, Sm, Eu) crystals, is given, in the standard notation [7], as follows:

$$H = g_{\parallel}\mu_B B_Z S_Z + g_{\perp}\mu_B(B_X S_X + B_Y S_Y) + \frac{1}{3}\sum_{m=0,\pm2} b_2^m O_2^m + \frac{1}{60}\sum_{m=0,\pm2,\pm4} b_4^m O_4^m$$

Table 1. Phase-transition temperatures and natures of phase transitions as deduced from EPR spectra in the 4.2–295 K temperature range. I and II in the brackets after the temperature indicate first- and second-order phase transitions, respectively. For the case of second-order phase transitions occurring above 200 K, the exponent β describing the variation of the EPR line position in the vicinity of the phase transitions, as calculated using equation (2), has been included; the experimental uncertainties enable determination of β to the first decimal place only.

Samples	Phase-transition temperature (K) (nature of phase transition)			
$RbPr(SO_4)_2.4H_2O$	261.0[a] (II, $\beta = 0.5$)	207.5[a] (II, $\beta = 0.5$)	175.0[a] (I)	71.4[b] (II), 9.7[b] (II)
$RbNd(SO_4)_2.4H_2O$	250.0[a] (II, $\beta = 0.5$)	219.5[a] (II, $\beta = 0.5$)	178.5[a] (I)	72.1[b] (II)
$RbSm(SO_4)_2.4H_2O$	—	232.0[a] (II, $\beta = 0.5$)	—	70.3[b] (II)
$RbEu(SO_4)_2.4H_2O$	—	230.5[a] (II, $\beta = 0.5$)	—	79.4[b] (II)
$RbEr(SO_4)_2.4H_2O$	—	228.1[b] (II, $\beta = 0.5$)	—	68.8[b] (II)
$RbDy(SO_4)_2.4H_2O$	260.3[b] (II, $\beta = 0.5$)	226.9[b] (II, $\beta = 0.5$)	—	65.4[b] (II)

[a] Reported by Misra and Misiak [7].
[b] Present work.

Table 2. The spin-Hamiltonian parameters (SHPs) for Gd^{3+}-doped $RbR(SO_4)_2.4H_2O$ crystals (R = Er, Dy) at site I at room temperature. The parameters b_1^m are in GHz. The root mean square deviation per line RMSL (GHz) $= \sqrt{\sum_i (\Delta E_i - h\nu_i)^2/n}$, where the summation is over the n line positions fitted simultaneously to estimate SHPs. ΔE_i and ν_i are the separation of the energy levels participating in resonance for the ith line position and the corresponding frequency of the microwave radiation, respectively; h is Planck's constant. The absolute sign of b_2^0 has been assumed positive in the absence of a liquid-helium-temperature spectrum with the same symmetry at room temperature; it is noted that the least-squares-fitting procedure yields correct relative signs of all b_1^m.

SHP	$RbDy(SO_4)_2.4H_2O$	$RbEr(SO_4)_2.4H_2O$
$g_\parallel$	2.004 ± 0.001	2.051 ± 0.001
$g_\perp$	1.995 ± 0.001	1.992 ± 0.001
b_2^0	0.397 ± 0.002	0.421 ± 0.002
b_2^2	-0.155 ± 0.002	-0.231 ± 0.002
b_4^0	-0.005 ± 0.001	0.051 ± 0.001
b_4^2	-0.059 ± 0.001	-0.042 ± 0.001
b_4^4	-0.040 ± 0.001	0.043 ± 0.001
b_6^0	-0.001 ± 0.001	0.032 ± 0.001
b_6^2	0.025 ± 0.001	-0.022 ± 0.001
b_6^4	0.048 ± 0.001	-0.021 ± 0.001
b_6^6	0.024 ± 0.001	-0.016 ± 0.001
RMSL	0.006	0.008
n	308	301

$$+\frac{1}{1260}\sum_{m=0,\pm2,\pm4,\pm6} b_6^m O_6^m. \tag{1}$$

The room-temperature spin-Hamiltonian parameters for $RbR(SO_4)_2.4H_2O$, R = Dy and Er, were estimated by the use of a rigorous least-square fitting technique utilizing numerical diagonalization of the 8×8 Gd^{3+} spin-Hamiltonian matrix [10]. All fine-structure resonant line positions as observed for many orientations of the external magnetic field were simultaneously fitted to evaluate the spin-Hamiltonian parameters, as listed in table 2. (The

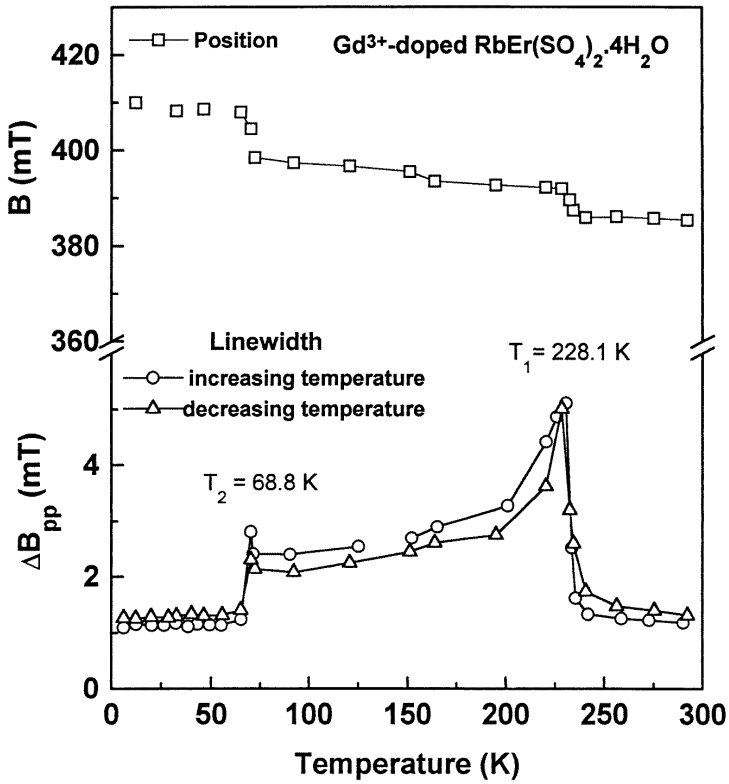

Figure 4. The position and width of the highest-field Gd^{3+} EPR lines at X band (∼9.60 GHz) K as functions of temperature for the external magnetic field orientation being parallel to the Z-axis in $RbDy(SO_4)_2.4H_2O$ in the 4.2–295 K temperature range.

values of the parameters $b_1^{-|m|}$ are too small, and not included in table 2.)

4. Theory and mechanisms responsible for second-order phase transitions in $RbR(SO_4)_2.4H_2O$ (R = Er, Dy)

According to Landau's theory of second-order phase transitions [11, 12], the free-energy density can be expressed in the temperature range close to T_c as a power series in the order parameter $Q \sim (T - T_c)^{\beta}$, with $\beta = 0.5$. As discussed by Misra and Shrivastava [13] the polarization of the surrounding ions determines the SHP of a paramagnetic ion, see e.g. calculations based on the point-charge and induced-dipole model [14, 15]. Thus, the shift in the positions of the EPR lines $\delta B = (B - B_{Tci})$ with temperature can be considered as the order parameter of the critical phenomenon, responsible for phase transition, in the vicinity of the phase-transition temperature, given by

$$\delta B \approx (T - T_c)^{\beta}. \tag{2}$$

The estimated values of β using experimental shifts, taking into account experimental uncertainties, are $\beta = 0.5$ at $T_c = 228.1$ K for $RbEr(SO_4)_2.4H_2O$ and at both $T_c = 260.3$ K and 226.9 K for $RbDy(SO_4)_2.4H_2O$. Good agreement between the values of β as estimated

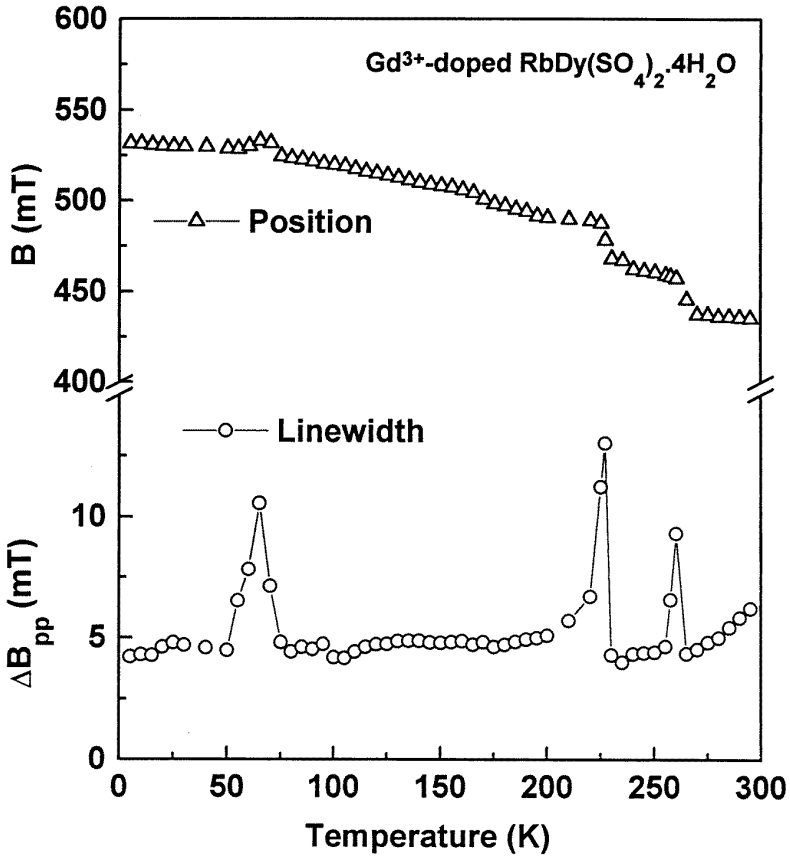

Figure 5. X-band (∼9.60 GHz) Gd^{3+} EPR spectra at selected temperatures for the orientation of the external magnetic field $\boldsymbol{B} \parallel Y$-axis in $RbPr(SO_4)_2.4H_2O$ single crystals at various temperatures in the 4.2–110 K temperature range to show the changes when the temperature is lowered.

here from EPR data in $RbEr(SO_4)_2.4H_2O$ and $RbDy(SO_4)_2.4H_2O$ using Landau's theory of second-order phase transitions is found to be in conformity with the exactly solvable spherical model as discussed by Misra and Shrivastava [13], for which $\beta = 0.5$, $\gamma = 2$ and $\delta = 5$ for the spatial dimension $d = 3$ [16, 17]. This is in accordance with the second-order phase transitions undergone by $RbR(SO_4)_2.4H_2O$ (R= Pr, Sm, Eu, Nd) as discussed in [7].

Using the calculated magnetic field values for the various transitions [18] from the eigenvalues estimated to second order in perturbation, one can express the shift in the position of a line below T_c as follows [13]:

$$\Delta B = \sum_i C_i \Delta a_i \tag{3}$$

where the Δa_i represent the differences of the respective SHP below T_c and C_i are constants. In writing equation (3), it has been assumed that C_i remain constant below T_c, which is true for second-order phase transitions where the changes are gradual. From equation (3) it is clear that those SHP which are most susceptible to structural changes, e.g. those with larger $|m|$ values, will be most sensitive to detect phase transitions by monitoring their values as

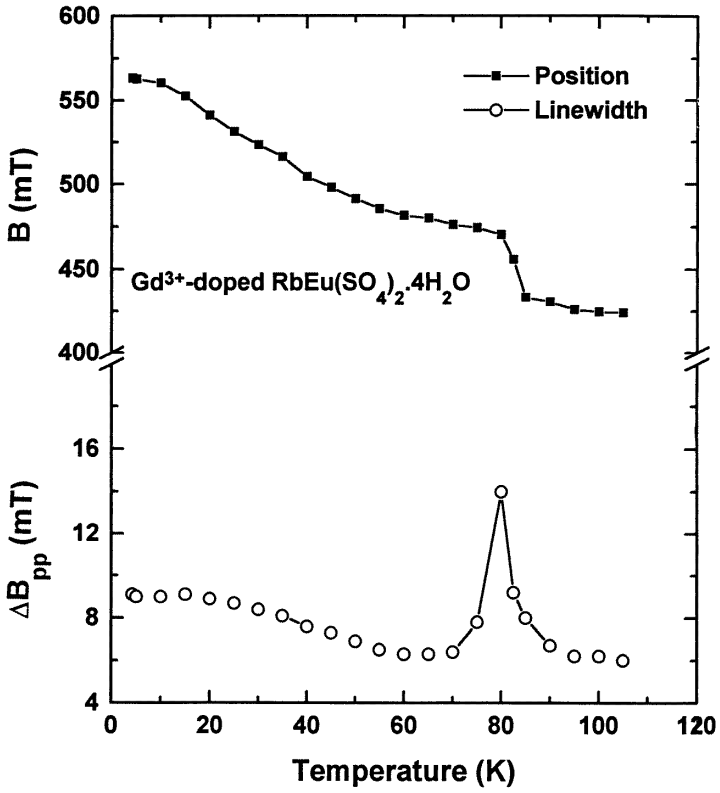

Figure 6. The position and width of the highest-field Gd^{3+} EPR line at X-band (∼9.60 GHz) as functions of temperature for the external magnetic field orientation parallel to the *Y*-axis in $RbEu(SO_4)_2.4H_2O$ in the 4.2–110 K temperature range.

functions of temperature. As for the EPR spectrum, this is reflected in the positions and widths of EPR lines as exploited in the present study.

The mechanism responsible for the occurrence of second-order phase transitions in $RbR(SO_4)_2.4H_2O$ is either rotation of distorted SO_4 tetrahedra, or order–disorder transition as discussed by Baker *et al* [17]. The sulphate tetrahedra play a more important role in the phase transition than do the water molecule, as they supply more (six) coordination oxygens to R^{3+} ions than the water molecules (three).

5. Systematics of phase transitions in $RbR(SO_4)_2.4\ H_2O$ and zero-field splitting parameters b_2^0 and b_2^2 (R = Pr, Nd, Sm, Eu, Dy, Er)

An inspection of table 1 reveals that all the six crystals undergo second-order phase transitions in the temperature range 207–232 K, and first-order phase transitions, except for the crystal with R = Dy, in the 65–80 K temperature range. In addition, the crystals with R = Pr, Nd, Dy experience another second-order phase transition in the temperature range 250–261 K, while there occurs one more second-order phase transition in the temperature range 175–178 K in each of the crystals with R = Pr, Nd. Summarizing, one can say that the two crystals with the lightest rare-earth ions, R = Pr, Nd, experience a total of

five and four phase transitions, respectively, two each of second-order and three and two, respectively, of first order, in the 4.2–295 K range, while the crystals with the heavier rare-earth ions (R = Sm, Eu, Dy, Er) each experience two phase transitions, one of first and the other second order, with the exception of the crystal with R = Dy, which experiences one more phase transition of second order at 260.3 K and undergoes a second-order phase transition at 68.8 K instead of a first-order one as compared to those occurring in all the other crystals. Thus, the rare-earth ions do play a significant role in the dynamics of phase transitions in $RbR(SO_4)_2.4H_2O$. However, since, in general, the temperatures of occurrence of corresponding transitions in the various hosts lie in close ranges, their effect does not appear to be as prominent as that of sulphate ions as discussed in section 4.

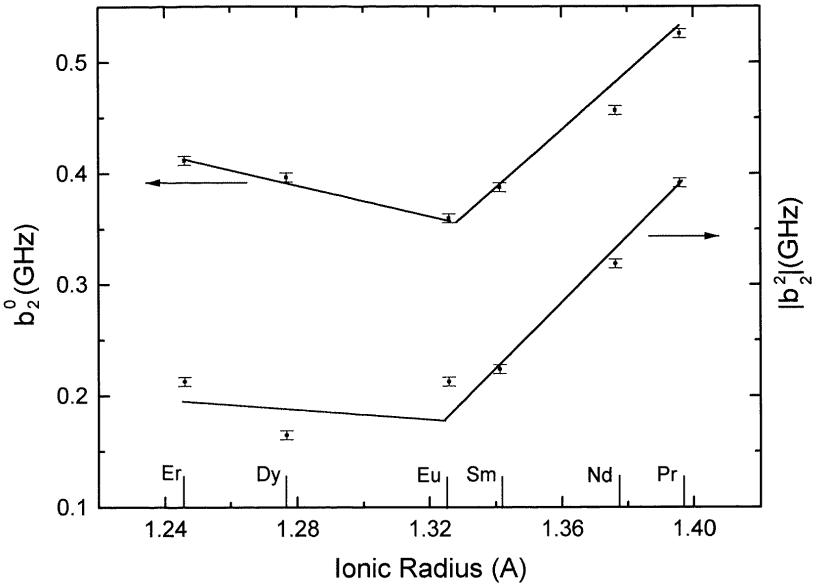

Figure 7. The magnitudes of the Gd^{3+} zero-field splitting parameters b_2^0 and b_2^2 (GHz) versus rare-earth ion radius in $RbR(SO_4)_2.4H_2O$ (R = Pr, Nd, Sm, Eu, Dy, Er). The straight lines are drawn to aid the eye, and do not represent least-squares fit to data points. (The ionic radii are taken from Shanon R D and Prewitt C T, 1970 *Acta Crystallogr.* B **26** 1046.)

As for the Gd^{3+} zero-field splitting parameters, the magnitudes of both b_2^0 and b_2^2 increase linearly in going to higher or lower rare-earth radius from those for the Eu^{3+} ion as shown in figure 7. This implies that the smaller the electronic spin of the rare-earth ion in $RbR(SO_4)_2.4H_2O$ the greater is the magnitude of b_2^0 or b_2^2, noting that the number (n) of 4f electrons and spin (S) of the various rare-earth ions are as follows: Pr^{3+} ($4f^2$, $S = 1$), Nd^{3+} ($4f^3$, $S = 3/2$), Sm^{3+} ($4f^5$, $S = 5/2$), Eu^{3+} ($4f^6$, $S = 3$), Dy^{3+} ($4f^9$, $S = 5/2$), Er^{3+} ($4f^{11}$, $S = 3/2$). (Here the electronic spin is calculated using Hund's rule.) This behaviour is almost but not entirely consistent with the prediction of the superposition model which dictates that the absolute value of a parameter increases with increase in the metal–ligand distance when the parameter t_2 is positive. On the other hand, the predictions on the basis of point-charge and induced-dipole models may be at variance with this as discussed in [14] and [15].

6. Concluding remarks

The salient futures of the present Gd^{3+} EPR study, focused on studying the systematics of the phase transitions and Gd^{3+} zero-field splitting parameters in the family of isostructural crystals $RbR(SO_4)_2.4H_2O$ (R=Er, Dy, Pr, Nd, Eu, Sm) over the entire range 4.2–295 K, are as follows:

(i) All the phase transitions undergone by the various host crystals are second order in nature, and are in accordance with Landau's theory of second-order transition (critical index $\beta \approx 0.5$), except for the crystals with R = Pr, Nd which undergo a first-order transition at 175.0 K and 178.5 K, respectively.

(ii) The Gd^{3+} spin-Hamiltonian parameters in the crystals with R = Dy, Er have here been estimated at room temperature. Combining the values in the other crystals (R = Pr, Nd, Sm, Eu), it is concluded that the magnitudes of the parameters b_2^0 and b_2^2 increase linearly as the radius of the rare-earth ion is either increased or decreased starting from that of Eu^{3+}, implying that the magnitudes of the parameters b_2^0 and b_2^2 decrease with increasing spin of the rare-earth ion.

(iii) As discussed in sections 4 and 5, these are the sulphate ions which appear to be most effective in the processes leading to phase transitions, although the R^{3+} ions and H_2O molecules do also play important roles in the dynamics of phase transitions.

It is hoped that this study will stimulate further studies leading to a better understanding of the critical behaviours exhibited by $RbR(SO_4)_2.4H_2O$ (R = Er, Dy, Pr, Nd, Eu, Sm), involving other techniques, e.g. infrared reflectivity, specific heat, x-ray, neutron scattering and nuclear magnetic resonance. As well, it will provide motivation to study other isostructural crystals $RbR(SO_4)_2.4H_2O$ not addressed so far.

Acknowledgments

This work was financially supported, in part, by the Natural Sciences and Engineering Council of Canada (S K Misra; grant No OGP 0004485). Thanks are due to Dr L Misiak for growing the crystals.

References

[1] Misra S K and Misiak L 1993 *Phys. Rev.* B **48** 13 578
[2] Martins G B, Pires M A, Barberis G E, Rettori C and Torikachvili M S 1994 *Phys. Rev.* B **50** 14 822
[3] Isber S, Charar S, Fau C, Mathet V, Averous M and Golacki Z 1995 *Phys. Rev.* B **51** 15 578
[4] Neogy D, Purohit T and Chatterjee A 1986 *J. Appl. Phys.* **59** 1272
[5] Trokiner A, Man P P, Theveneau H and Papon P 1985 *Solid State Commun.* **55** 929
[6] Jasty S and Malhotra V M 1992 *Phys. Rev.* B **45** 1
[7] Misra S K and Misiak L E 1997 *Phys. Rev.* B **55** 2391
[8] Malhorta V M, Bist H D and Upreti G C 1974 *Chem. Phys. Lett.* **28** 390
[9] Misra S K, Li X, Misiak L E and Wang C 1990 *Physica* B **167** 209
[10] Misra S K 1976 *J. Magn. Reson.* **23** 403
Misra S K and Subramanian S 1982 *J. Phys. C: Solid State Phys.* **15** 7199
[11] Smolenski G A, Bkov V A, Isaapov V A, Krainik N N, Pasykov R E and Salokov A I 1984 *Ferroelectrics and Related Materials* ed G A Smolenski (New York: Gordon and Breach)
[12] Lines M E and Glass A M 1973 *Principles and Applications of Ferroelectrics and Related Materials* (Oxford: Clarendon)
[13] Misra S K and Shrivastava K N 1988 *Phys. Rev.* B **33** 2255
[14] Lewis N R and Misra S K 1982 *Phys. Rev.* B **25** 5421
[15] Lewis N R and Misra S K 1983 *Phys. Rev.* B **27** 3425
[16] Wortis M 1973 *Proc. Conf. on Renormalization Group (Chestnut Hill, PA)* ed G D Gunton and M S Green (Philadelphia, PA: Temple University Press)
[17] Baker G A Jr, Gilbert H E, Eve J and Rushbrooke G S 1967 *Phys. Rev.* **176** 739
[18] Abragam A and Bleaney B 1970 *Electron Paramagnetic Resonance of Transition Ions* (Oxford: Clarendon)